

## Behavior of Lightweight Concrete Under Uniaxial Eccentric Compressive Stresses

\*Maged Tawfik<sup>1</sup>, Sherif Elwan<sup>2\*</sup>, Hosam Seleem<sup>3</sup>, Amr Abdelrahman<sup>4</sup>

<sup>1</sup> Research Assistant, Structural Engineering Department, Ain Shams University, Cairo, EGYPT

<sup>2</sup> Associate Professor, Department of Civil Eng., The Higher Institute of Engineering, El Sherouk City, Cairo, Egypt

<sup>3</sup> Professor, properties and Strength of Materials, Building National Research Center, Cairo, EGYPT

<sup>4</sup> Professor, Concrete Engineering Department, Ain Shams University, Cairo, EGYPT

Corresponding author: \*Maged Tawfik

---

**ABSTRACT:** This paper presents an experimental investigation for the behavior of reinforced lightweight concrete (LWC). LWC was obtained through the use of polystyrene foam as a partial aggregate's replacement to reduce the concrete dry unit weight from 23.0 kN/m<sup>3</sup> to 18.1 kN/m<sup>3</sup>. The experimental work was consisted from two phases; the first phase was aimed to determine the LWC stress block parameters and the second phase was concerned with the behavior of reinforced LWC columns under eccentric load.

In order to determine the stress-strain distribution of LWC and evaluate various parameters of the rectangular stress block, Square half-scale column specimen with dimension 200 x 200 mm and 1600 mm height was tested. It had two arms, each of them was connected at the top and bottom ends of the specimen to transfer the moment from the applied load to specimen. For the second phase, six half scale LWC square specimens with different eccentric ratios (e/t) and different transverse reinforcement were tested under eccentric loads using the same dimensions as in the first phase.

Stress block parameters phase consists of two specimens were used to evaluate the flexural behavior of LWC results indicated that the stress block parameter k<sub>1</sub> is 0.61 when cylinder lightweight concrete compressive strength 30 MPa. The generalized stress block parameter k<sub>2</sub> is found to be equal 0.37, and the generalized stress block parameter k<sub>3</sub> is 1.12. From these values we found the stress block parameters  $\alpha_1$  and  $\beta_1$  equal 0.93 and 0.73 respectively. Phase two results have showed that increasing eccentricity ratio leads to increase LWC compression side strain value, reduce strain in the longitudinal reinforcement in tension side, reduce the transverse reinforcement strain. Increasing transverse reinforcement ratio leads to increase the failure load, and consequently increase the deformation and strain increases in the LWC compression side strain value, the longitudinal reinforcement strain, and the transverse reinforcement strain.

**Keywords:** Confinement; eccentricity; Lightweight concrete (LWC); polystyrene foam; Mixes; Stress block parameters.

---

### I. INTRODUCTION

Structural lightweight concrete mixtures can be designed to achieve similar strengths as normal weight concrete. The same is true for other mechanical and durability performance requirements. Structural lightweight concrete provides a more efficient strength-to-weight ratio in structural elements. In most cases, the marginally higher cost of lightweight concrete is offset by size reduction of structural elements, less reinforcing steel and reduced volume of concrete, resulting in lower overall cost could have impact on the design of the foundations. Use of reduced unit weight concrete could also lead to great advantages for the precast industry by reducing the transportation cost. Furthermore, the reduced mass will reduce the lateral load that will be imposed on the structure during earthquakes, hence simplifying and reducing the lateral load carrying system.

Large numbers of researchers have been working on the stress-strain distribution of concrete since the beginning of the 20th century. Hognestad et al. (1955) developed a test set-up and derived equations which were milestones in evaluation of the stress-strain relationship of concrete. In this test setup, the compression zone of a flexural member with a rectangular cross section is simulated by varying the axial load and the moment on the section. By many researchers, this test setup was referred to as Hognestad test setup and these specimens were referred to as "C-Shaped Specimens" or "Eccentric Bracket Specimens". This method formed the basis for the future research on determination of stress block parameters of concrete. For this purpose a total of 20 bracket specimens with cylinder concrete compressive strengths ranging from 0.775 to 7.61 ksi were tested under combined axial load and bending. The central unreinforced test region had a cross-section of 5x8 in. and was 16 in. long. The brackets were heavily reinforced to obtain a failure in the central unreinforced test region. The specimens were cast horizontally and tested vertically. The test method consisted of applying a major load, P<sub>1</sub>, using a testing

---

machine and a minor load, P2, that could be varied independently to maintain the neutral axis at the inner face of the test specimen throughout the test. This eliminated any complications resulting from tensile stresses in the concrete. The major load was applied at a constant rate from zero to failure. The minor load was applied using a hydraulic jack through one or two tie rods and varied throughout the test to obtain zero strain within  $\pm 5 \mu\epsilon$  at inner face of the specimen. Strains were measured using 6 in. strain gauges, two at the neutral surface, and two at the compression surface and one at mid-depth on each of the two side faces. The test duration was 15 minutes which corresponded to a rate of 3.1 to 4.2 micro strains per second on the compression face. Three or four 6×12 in. Concrete cylinders were tested with each specimen. The testing ages were 7, 14, 28 and 90 days. Test results indicated that the majority of the collected data for the generalized stress block parameter  $k_1$  was 0.9, 0.86, 0.82, 0.79, 0.75, 0.71, 0.67, 0.63  $K_2$  was equal 0.49, 0.48, 0.46, 0.45, 0.44, 0.42, 0.41, 0.40,  $k_3$  was equal 1.12, 1.03, 0.97, 0.94, 0.92, 92, 0.93, 0.94. This values for compressive strength 1000, 2000, 3000, 4000, 5000, 6000, 7000, 8000Psi respectively.

Halit Cenan Mertol (2006) has tested 21 plain concrete specimens under combined flexure and axial compression to evaluate the stress-strain distribution and stress block parameters of high strength concrete (HSC) in the compression zone of flexural members. The variables considered in this investigation were mainly the strength of concrete and the age of the specimen. A total of 42 cylindrical specimens and 18 prism specimens were used to evaluate the creep and shrinkage properties of HSC. His test concept was based on the test method developed by Hognestad et al. (1955) to simulate the compression zone of a flexural member. The two axial loads were adjusted during the test to maintain zero strain (which is at the neutral axis for a flexural member) at one face of the specimen and the maximum compressive strain at the opposite face of the cross-section. The main parameter was the concrete compressive strength ranging from 10.4 to 16 ksi. A total of forty two 4×12 in. cylindrical specimens and eighteen 3×3×11¼ in. prism specimens were monitored for one year. The variables considered in this investigation were the concrete compressive strength ranging from 10.4 to 16.7 ksi, specimen size (cylindrical or prism), curing type (moist or heat curing), age of concrete at loading (1, 7, 14, 28 days) and loading stress level (0.2f<sub>c</sub> or 0.4f<sub>c</sub>). His test results indicate that the majority of the collected data for the generalized stress block parameter  $k_1$  for HSC is higher than 0.58 for concrete compressive strengths ranging between 10 and 18 ksi. Therefore, using the lower bound of 0.58 is proposed for  $k_1$  parameter for concrete compressive strengths beyond 15 ksi, the value of  $k_3$  parameter was 0.85, and Poisson's ratio of 0.2 was found to be an appropriate value for concrete compressive strengths up to 18 ksi,  $k_2$  between 8 ksi and 18 ksi can be assumed to be 0.33.  $k_3$  parameter equal 0.85, for concrete compressive strengths up to 18 ksi is found to be appropriate for design purposes, and the stress block parameter  $\alpha_1$  equal 0.9,  $\beta_1$  equal 0.75.

Y.C. Kan, L.H. Chen. C.H. Wu, C.H. Huang , T. Yen, and W.C. Chen (2012) studied the behavior of LWC Columns under axial load. This research aims to figure out the behavior of axial load and size effect of reinforced lightweight aggregate concrete column. Both normal weight aggregate concrete (NWC) and lightweight concrete (LWC) were used to cast three similar square columns with various sizes. The slenderness ratio of all columns is 21.6. Two concrete compressive strengths of 23 and 33 MPa were selected. Test results revealed that the failure model of LWC columns is similar to that of NWC column. The tension crack appeared at the middle part of both concrete columns. Under the same axial loading, the displacement of LWC column is larger than that of NWC column. The measured ultimate strengths of the small- and medium-size LWC columns are close to the computed values of ACI nominal strength indicating that the ACI equation of nominal strength is quite applicable for the strength prediction of small-size and medium-size LWC columns. In addition, the ratio of (ultimate strength / nominal strength) of LWC column decreases with the increase of column size; when the strength of concrete increases, the ratio of (ultimate strength / nominal strength) decreases. These results indicate that LWC columns have the incentive of size effect. Therefore, the size effect should be considered in the design of LWC columns.

M. R. Esfahani and A. Kadhodaee (2008) studied strength and ductility of reinforced concrete columns made of lightweight aggregates under eccentric loading. In this research, the strength and ductility of reinforced concrete columns made of lightweight were tested. The shape and spacing of transverse reinforcement and compressive strength of specimens were varied. For all specimens, the eccentricity of axial loading was 60 mm. Test results showed that the confinement of transverse reinforcement has a positive effect on the ultimate strength and ductility. Test results have been compared with the provisions of ACI Code for normal strength concrete. The comparison shows that the reinforced concrete columns made of natural lightweight aggregates can be used in structures if they include appropriate transverse reinforcement and have a good mix design.

Hussein O. Okail (2008) explained a group of six medium scale beams coded N1, L1, L2, L3, L4, and L5, Beams had a rectangular cross-section of dimensions 150 mm x 300 mm over a total length of 3000 mm and a clear span of 2700 mm. Shear reinforcement was increased in the region outside the two concentrated loads near the support to clearly pronounces the parameters of the study, the flexural reinforcement ratio through beams L1, L4 and L5, having reinforcement ratios of 0.80%, 1.35% and 1.90%, respectively, Finally, the amount of stirrups located at the constant moment zone is discussed through beams L2, L1 and L3, having stirrups of zero, 5Φ8/m'

and  $10\Phi 8/m^2$ , respectively. In this respect and for ease and simplicity of calculations, the equivalent rectangular stress block [Whitney block, adopted in both ACI 318-02 (2002) and ECCS 203-01 (2001)] is used. The analysis also demonstrated that, for the latter block to have the well-established uniform, its stress block parameter  $\beta_1$  should be 0.72 the neutral axis depth,  $c$ . for all other parameters we make this research.

## II. TESTING PROGRAM

This section describes the experimental work performed through this study beginning with the used materials, specimen's details, measurement devices, test setup, and specimen's grouping.

### 2.1. Materials Used

All specimens are made from one concrete mix with the proportion shown in Table 1. The target standard 28-days compressive cube strength  $f_{cu} = 38\text{MPa}$ , and according to the ACI the equivalent compressive cylinder strength,  $f'_c = 30\text{ MPa}$ . The results of testing cubes have satisfied the target strength. Ordinary locally available concrete constituent materials have been used to manufacture the test specimens. The used silica fume consists of very fine vitreous particles with a surface area on the order of 20000 m<sup>2</sup>/Kg, The normal silica fume range from 5 to 20 percent of Portland cement content. The used polystyrene foam is type of plastic produced from styrene. Polystyrene foam has an excellent resistance to moisture, imperiousness to rot, mildew and corrosion. The used super-plasticizer was of a liquid form under trade name, VISCOCONCRETE#3425 which is in compliance with ASTM C494, 2001 of type V with dose of cement about 3%. It permits a reduction of 30% of the water content in concrete mixture.

The reinforcement used in the specimens consisted of longitudinal and transverse reinforcement, High grade steel for 10mm and 12mm diameter were implemented. The average tensile yield strength ( $f_y$ ) was 460 MPa, the ultimate strength ( $f_u$ ) was 530 MPa and the modulus of elasticity ( $E_s$ ) 193 GPa. Mild steel for 8mm diameter was implemented with average tensile yield strength ( $f_y$ ) was 280 MPa, the ultimate strength ( $f_u$ ) was 460 MPa and the modulus of elasticity ( $E_s$ ) 117 GPa.

Polypropylene MasterFiber@012(BASF product) is used by 19mm length for plastering at the rate of 0.9kg/m<sup>3</sup>, with tensile strength 350N/mm<sup>2</sup>.

### 2.2. Specimens Details

The specimens used in phase one have square cross section with dimensions 200x200 and 1600mm height. The end sections of the concrete specimen was reinforced with three U-shaped longitudinal (3Φ12) and four transverse reinforcement (4Φ10) to transfer the moment from the arms to the concrete specimen. A general view of the phase one specimen shown in Fig.1-a.

Six specimens in phase two were divided into two groups with longitudinal reinforcement 4Φ10 with ratio to concrete cross section 0.8% used for all specimens as shown in Fig.1-b The first group have stirrups Φ8 with ratio 0.4% and the second group have stirrups Φ10 with ratio 0.6%, All columns have square cross section with dimension 200x200mm and 1600mm height, Specimens have column head with dimensions 400x200mm and tapered depth from 100 to 200mm, as shown in Fig.1-b. The coding, concrete dimensions, reinforcement details, and eccentricity ratios of the aforementioned columns are also summarized in Table 2.

Table 1: Mix design proportion / m<sup>3</sup> (Average Strength= 38 MPa)

Group	ID	Cross section (mm)	Specimens height (mm)	Longitudinal Reinforcement	Transverse Reinforcement	Eccentricity/Thickness (e/t)
(A)	C1	200x200	1600	4 Φ 10	Φ 8@200mm	0
	C2	200x200	1600	4 Φ 10	Φ 8@200mm	0.2
	C3	200x200	1600	4 Φ 10	Φ 8@200mm	0.4
(B)	C4	200x200	1600	4 Φ 10	Φ 10@200mm	0
	C5	200x200	1600	4 Φ 10	Φ 10@200mm	0.2
	C6	200x200	1600	4 Φ 10	Φ 10@200mm	0.4

Table 2: Specifications of the tested columns on phase two.

### 2.3. Measuring Devices

Cement ( Kg)	Silica Fume ( Kg)	Coarse Agg. ( Kg)	Sand ( Kg)	Polystyrene Foam (Liter)	Super Plasticizer (Liter)	Water (Liter)	Fiber (kg)
450	40	630	630	330	13.5	139	0.9

HPM electrical strain gauges of 10 mm length and 120 Ohm resistance were used to measure the steel and concrete strains throughout the test specimens. Eight HPM electrical strain gauges were used in phase one for measuring concrete compressive strain. Four in compression side and four in other side to make sure the strain in this side equal zero as shown in Fig.1-a. The location of HPM electrical strain gauges in phase two specimen are shown in Fig.1-b.

Linear Variable Displacement Transducers (LVDTs) were used to monitor the displacements throughout the tests. For phase two specimens, one LVDT with maximum gauge length of 100mm and precision of 1/100 mm were used to measure the deflection at 600 mm length, was used to measure axial deformation at mid. height for specimens in phase two as shown in Fig.1-b.

### 2.4. Test Setup

Test setup for phase one specimen has two steel moment arms connected to the ends of the specimen. Since the ends of the concrete specimen were confined with longitudinal and transverse reinforcement, the connection was established using threaded rods through the holes on the specimen and the steel arms. Two hinges were used to eliminate the end restrictions on the specimen. In bottom of hinge, steel plate with thickness 50 mm to make uniform distribution of load in specimens. The main axial load was applied using 5000 KN compression machine. The specimen was placed on the hinged support lying on the compression machine. Steel plate was used between the specimen and the hinged support both at the top and bottom to level the concrete specimen and to eliminate localized concrete failure at the ends. After performing necessary leveling, lumber was placed under the moment arm to hold everything in position. The secondary load which created flexural effects on the specimen was applied using a 500 KN hydraulic jack.

The load cell and the jack were positioned on the top moment arm and both arms were connected together by using threaded rod. The test setup of specimens in phase one is shown in Fig.1-a. Phase two specimens were instrumented to measure their mechanical behavior after each load increment using the following tools. Two steel confined plates were made at top and bottom level of concrete specimen and to eliminate localized concrete failures at the ends. Two hinges were used to eliminate the end restrictions on the specimen. In bottom of hinge, a steel plate with thickness 50 mm to make uniform distribution of load in specimens.

### III. EXPERIMENTAL TEST RESULTS

The experimental results including deflections, strains (for concrete and steel) and crack propagation were introduced at different stages of loading. Approaching the failure load level, any small change in the applied load resulted in a large deformation in the tested specimens. Therefore the concrete strain reading was difficult to be recorded at this load level (after maximum load) to insure safety of human and instruments. The crack pattern were also discussed and plotted at different stages of loading.

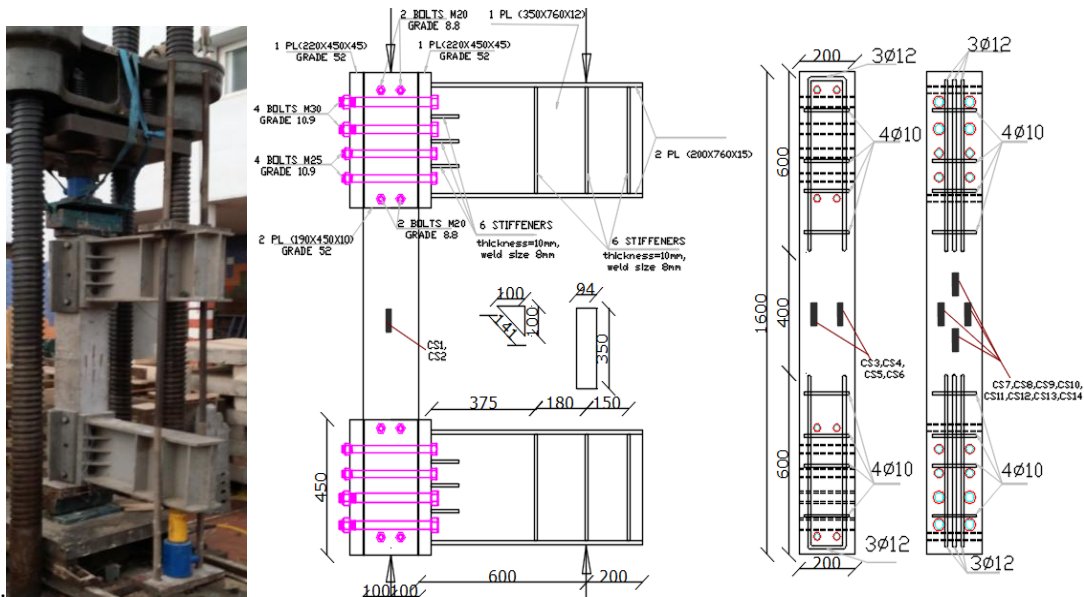


Fig.1-a: Test Setup of specimens in phase one

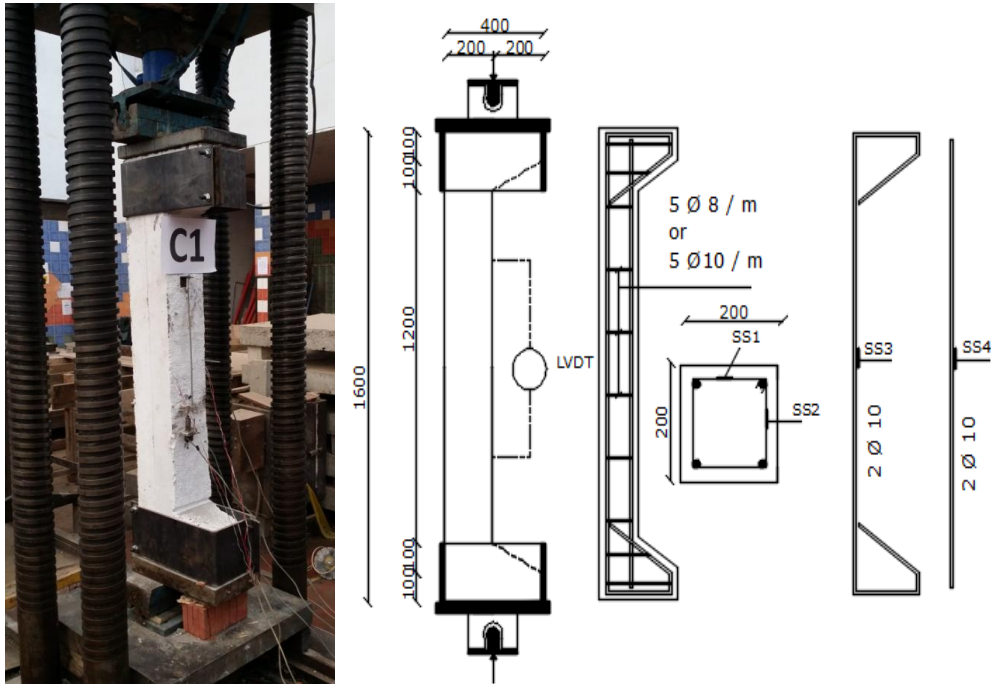


Fig.1-b: Test Setup of specimens in phase two

### 3.1. Stress block parameter Phase

At a main load level of 768.189 kN and secondary load of 35.646 kN, failure occurred due to crushing of concrete in the middle of compression side when the concrete strain reached the ultimate strain which equal 0.0018 for first specimen, and the second specimen gives main load level of 810.25 kN and secondary load of 37.156 kN, failure occurred due to crushing of concrete in the middle of compression side when the concrete strain reached the ultimate strain which equal 0.0017. Fig.2 and 3 shows the crushing of phase one specimen, and the value of average two specimens strain in tension and compression side of the specimen.



Fig.2: Crushing of the concrete of stress block parameter specimen.

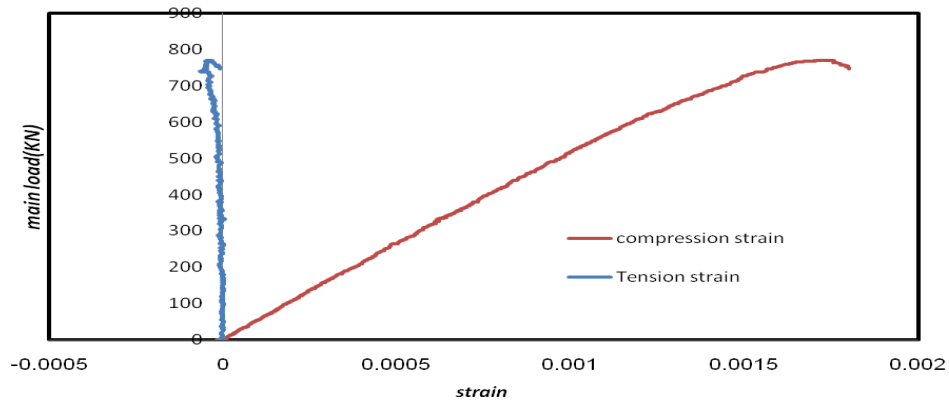


**Fig.3:** Average strain in concrete at tension and compression side of stress block parameter specimen.

The rectangular stress block was first proposed by von Emperger in 1904 (Mattock et al. 1961) and since that time this idea was improved by Hognestad et al. (1955) The rectangular stress block parameters  $\alpha_1$ , and  $\beta_1$  are used to determine the stress-strain relationship. This approach assisted to calculate the concrete stress,  $f_c$  as a function of measured strain at the most compressed fiber  $\epsilon_c$ , and the applied stresses  $f_o$  and  $m_o$ . The following equations were obtained from equilibrium of external and internal loads and moments. Note that the eccentricities due to deflection of the member were also considered in the calculation of applied moment,  $M$ .

$$C = P_1 + P_2 = f_o bc \quad (1)$$

$$M = P_1 a_1 + P_2 a_2 = m_o bc^2 \quad (2)$$

where,  $C$  is the total applied load,  $M$  is the total applied moment,  $P_1$  is the main axial load,  $P_2$  is the secondary load,  $a_1$  and  $a_2$  are the eccentricities,  $b$  is the width of the section,  $c$  is the depth of neutral axis are shown in Fig.4.

$$f_o = (P_1 + P_2) / bc \quad (3)$$

$$m_o = (P_1 a_1 + P_2 a_2) / bc^2 \quad (4)$$

Differentiating the last terms of the equations for  $C$  and  $M$  with respect to would  $\epsilon_c$  would yield the following equations.

$$\sigma_{c1} = \epsilon_c (df_o / d\epsilon_c) + f_o \quad (5)$$

$$\sigma_{c2} = \epsilon_c (dm_o / d\epsilon_c) + m_o \quad (6)$$

Using these equations, two similar stress-strain relationships were obtained for each eccentric bracket specimens, stress-strain relationship of LWC specimens are shown in Fig.5.

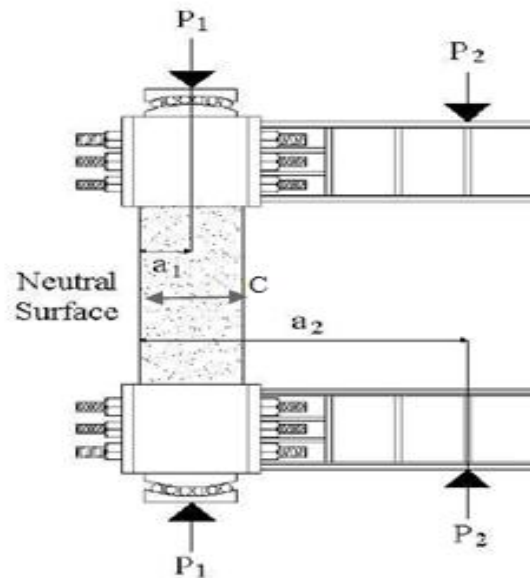


**Fig 4:** Applied Forces on Eccentric Bracket Specimens



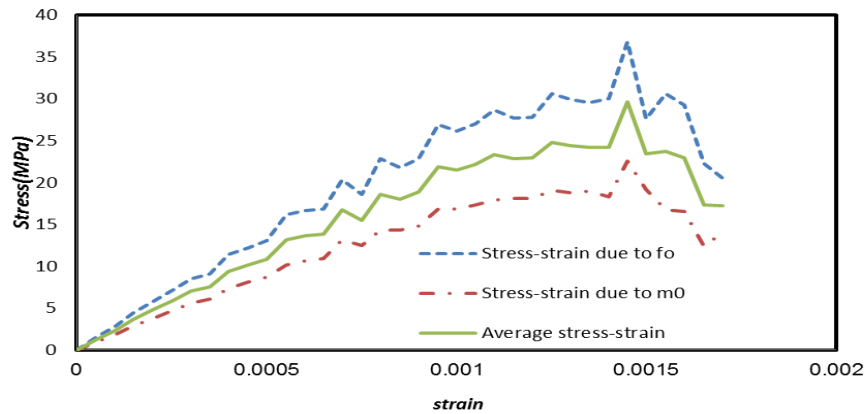


Fig.5: Two Similar Stress-Strain Relationships for first specimen.

Stress-strain relationships obtained from eccentric bracket specimens were used to calculate the generalized and rectangular stress block parameters for LWC. The values of  $k_1$ ,  $k_2$ , and  $k_3$  can be obtained from the equilibrium of the external and internal forces, as follows:

$$k_3 = \sigma_{max} / f_c' \quad (7)$$

$$P_1 + P_2 = k_1 k_3 f_c' bc \quad (8)$$

$$k_1 k_3 = (P_1 + P_2) / f_c' bc \quad (9)$$

$$k_2 = 1 - (P_1 a_1 + P_2 a_2) / (P_1 + P_2) x c \quad (10)$$

$$C = \alpha_1 \beta_1 f_c' bc = k_1 k_3 f_c' bc \quad (11)$$

Therefore

$$\alpha_1 = k_1 k_3 / 2 k_2 \quad (12)$$

$$\beta_1 = 2 k_2 \quad (13)$$

Test results indicate that the generalized stress block parameter  $k_1$  is 0.61 when cylinder lightweight concrete compressive strength 30 MPa. The generalized stress block parameter  $k_2$  is found equal 0.37. The generalized stress block parameter  $k_3$  for LWC is determined to be similar to NSC and it is equal 1.12, from these values we found the stress block parameters  $\alpha_1$  equal 0.93 and  $\beta_1$  equal 0.73.

### 3.2. Eccentric loading Phase

The results obtained from uniaxial eccentric compression tests conducted on the columns and strains at concrete, longitudinal reinforcement (compression side, tension side) and transverse reinforcement are summarized in Table 3 for first crack stage and failure stage.

Table3 Summarized strains on specimens at first crack stage and maximum Load stage.

I.D	At First Crack					At Maximum Load				
	Crack Load (K.N)	Concrete Strain $\times 10^{-6}$	Long. Rft. strain at inner side $\times 10^{-6}$	Long. Rft. Strain at outer side $\times 10^{-6}$	Long. Rft Strain at outer side $\times 10^{-6}$	Failure Load (K.N)	Concrete Strain $\times 10^{-6}$	Long. Rft. strain at inner side $\times 10^{-6}$	Long. Rft Strain at outer side $\times 10^{-6}$	Long. Rft Strain at outer side $\times 10^{-6}$
C1	960.1	-1018	-1200	-1150	294	1207	-170	-168	-160	382.4
C2	473.4	-1080	-1000	-820	185	712.1	-210	-163	-121.5	350
C3	220.2	-1050	*****	670	176	367.3	-198	*****	105	315.3
C4	1012	-1034	-1280	-1231	296	1350	-182	-181.8	-175.2	446.6
C5	501.8	-1112	-1150	****	195	780.7	-223	-172	*****	390
C6	340.2	-1090	-1120	768	180	445.7	-205	-165	134	360

\*\*\*\*\* Strains cannot be determined because of strain gauges damage during casting

#### 3.2.1. Failure Patterns

For axially loaded columns (C1&C4) the initiation of cracking and crushing occurred at zone near the lower middle of column, The failure was associated with concrete crushing near the column ends, This may attributed to the high concentration of stresses near the column head, as shown in Fig.6-a, and Fig.6-b Columns

(C2&C3&C5&C6) tested under static monotonic uni-axial loading, the initiation of cracking and crushing occurred at the middle height of column, When the eccentricity ratio ( $e/t$ ) increased the cracking width increased and the failure was crushing failure at the middle height of column with wide cracks in the tension side, and when we increased the transverse reinforcement ratio crack width decreased and late appearance of first crack in column, as shown in Fig.6-a, and Fig.6-b.

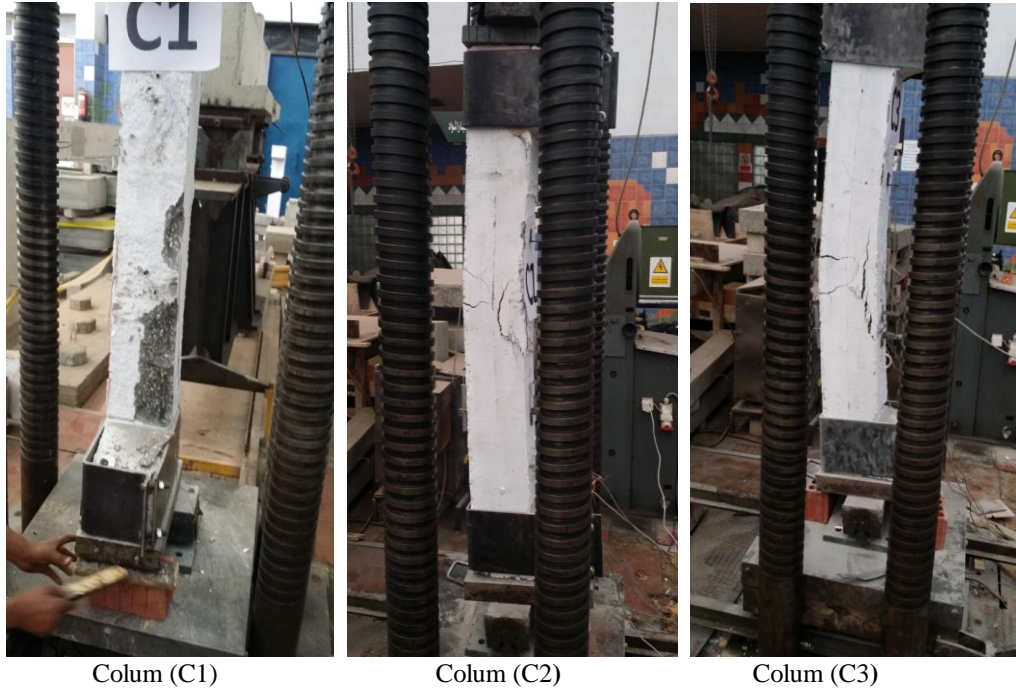


**Fig.6-a:** Crushing of group (a) specimens in eccentric loading phase.

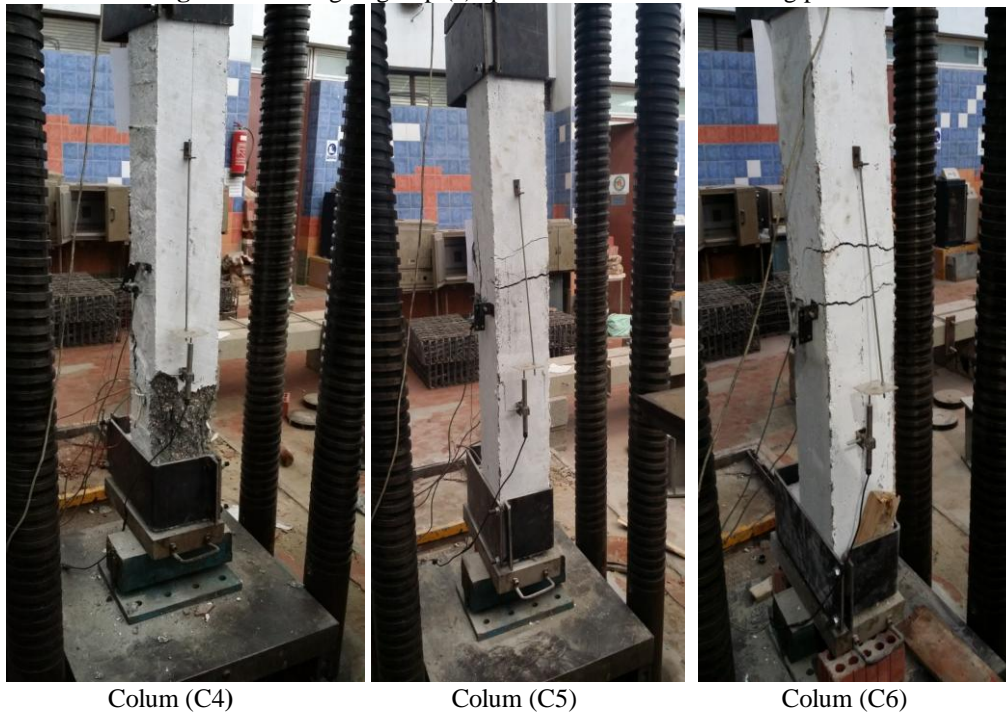


**Fig.6-b:** Crushing of group (b) specimens in eccentric loading phase.



3.2.2 Failure loads and strains compression

**Table 4:** Summarized percentage of changes in all parameters for tested columns.

Comparison Type	Group	I.D.	Percent of changing at Maximum Load%				
			Failure Load	Concrete Strain	Long. RFT strain at inner side (comp.)	Long. RFT Strain at outer side (tension)	Trans. RFT. Strain
Results of eccentric columns	Group (A)	C2	-40.10%	23.50%	-3.0%	-92.40%	-8.47%
		C3	-69.60%	16.50%	----	-165.6%	-17.50%
Results of concentric column(e/t=0)	Group (B)	C5	-42.20%	18.4%	-5.40%	---	-12.70%
		C6	-67.0%	12.60%	-9.20%	-162.4%	-19.40%
Results of columns with transverse reinforcement 0.6%	e/t=0	C4	11.90%	7.60%	8.20%	9.50%	-16.80%
	e/t=0.2	C5	9.60%	6.20%	5.50%	---	-11.40%
Results of columns with transverse reinforcement 0.4%	e/t=0.4	C6	21.4%	3.53%	---	27.60%	-14.17%

Some strains for phase two specimens cannot be determined because of electrical strain gauges damage during casting. When the eccentricity ratio increased the load decreased but the moment increased with ratio more than load decreased and it leads to increase LWC compression strain value, The reason of reduce strain in the longitudinal reinforcement in inner side with increasing eccentricity ratio was changes the magnitude of moment in the bars less than the magnitude of moment in the external fiber of LWC with the same load, The transverse reinforcement strain is reduced when the eccentricity ratio increased because when the eccentricity ratio increased the buckling of longitudinal bars decreased and it leads to decrease the deformation and strain of transverse reinforcement. The changes in transverse reinforcement bar diameter between 8mm (0.4%), 10 mm (0.6%) results in more confinement and it leads to increase the failure load, when the load increased the deformation increased and all strains increased.

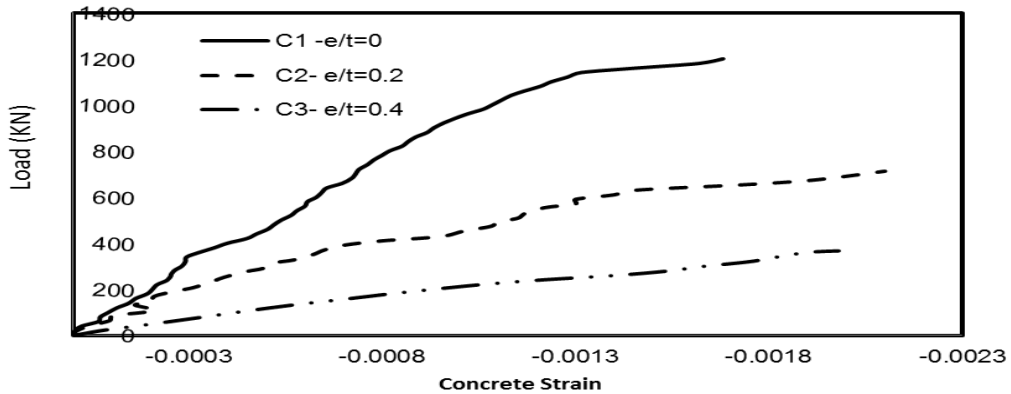


Fig.7: Load-Concrete Strain curve for columns with transverse reinforcement having ratio of 0.4%.

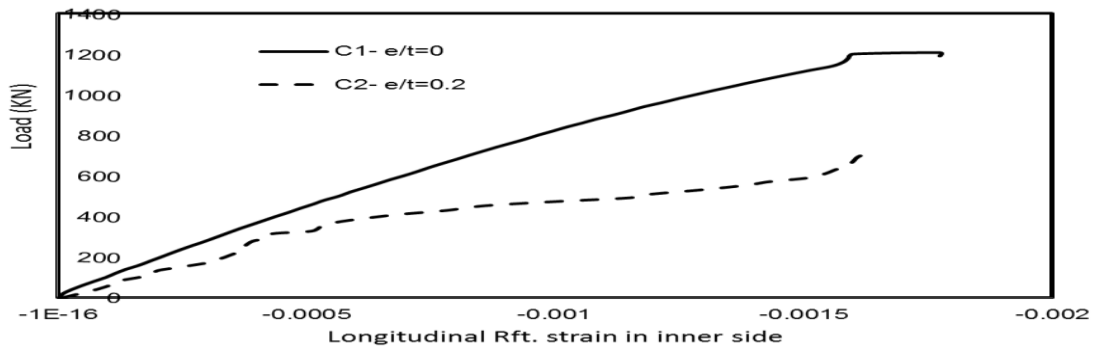
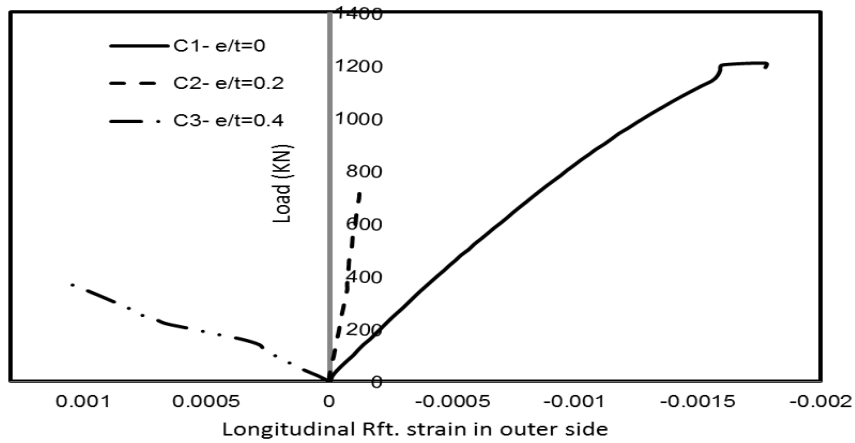
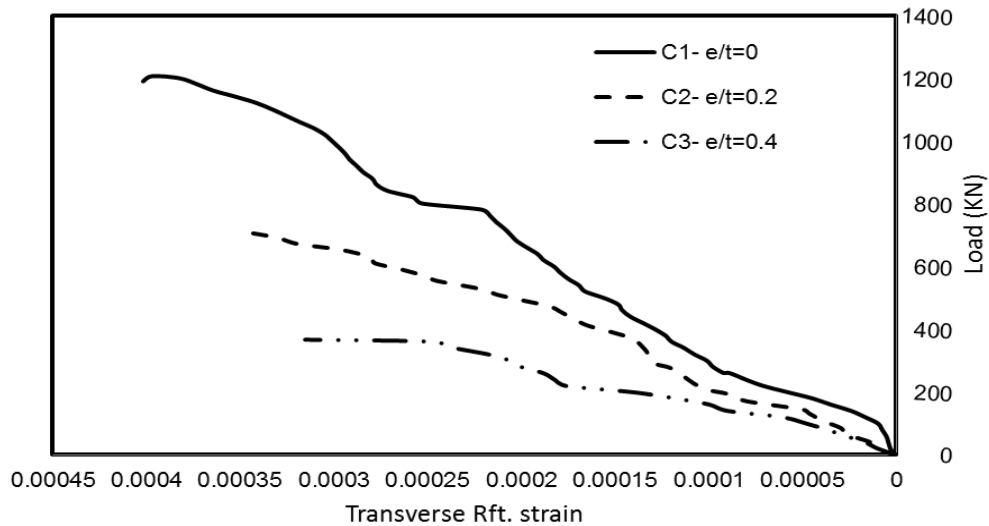


Fig.8: Load -longitudinal reinforcement Strain at inner side curve for columns with transverse reinforcement having ratio of 0.4%.



**Fig.9:** Load -longitudinal reinforcement Strain at outer side curve for columns with transverse reinforcement having ratio of 0.4%.



**Fig.10:** Load -transverse reinforcement strain curve for columns with transverse reinforcement having ratio of 0.4%.

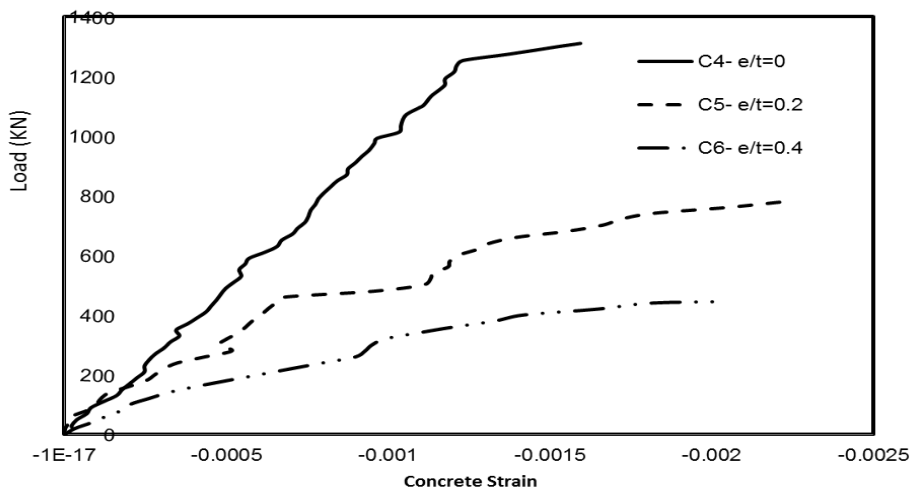


**Fig.11:** Load-Concrete strain curve for columns with transverse reinforcement having ratio of 0.6%.

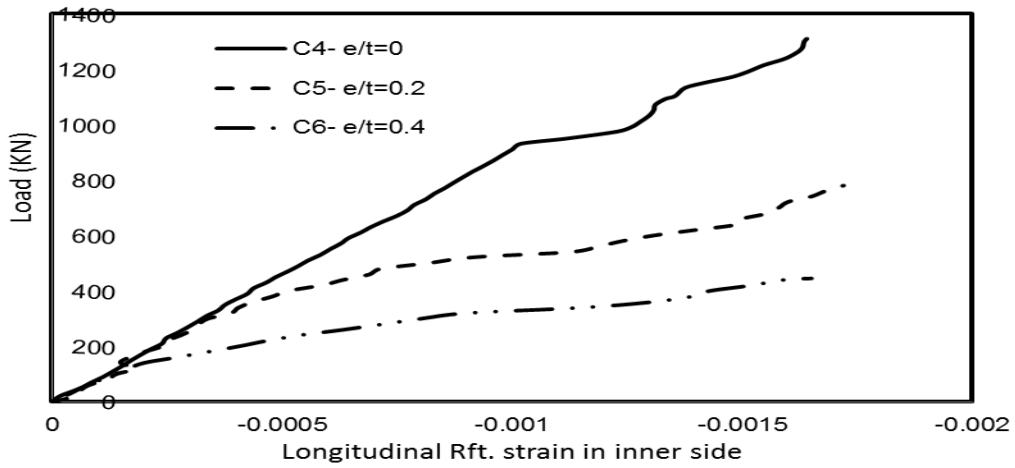


**Fig.12:** Load -longitudinal reinforcement strain at inner side curve for columns with transverse reinforcement having ratio of 0.6%.

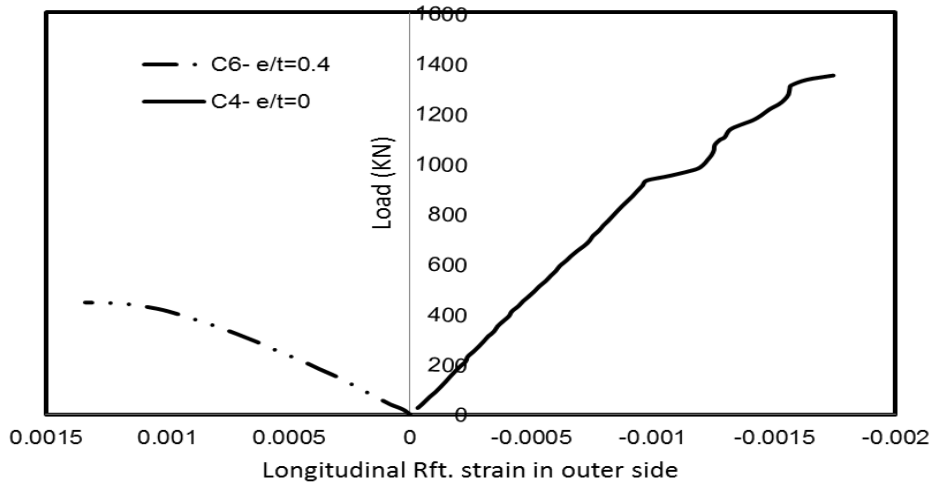


**Fig.13:** Load -longitudinal reinforcement strain at outer side curve for columns with transverse reinforcement having ratio of 0.6%.

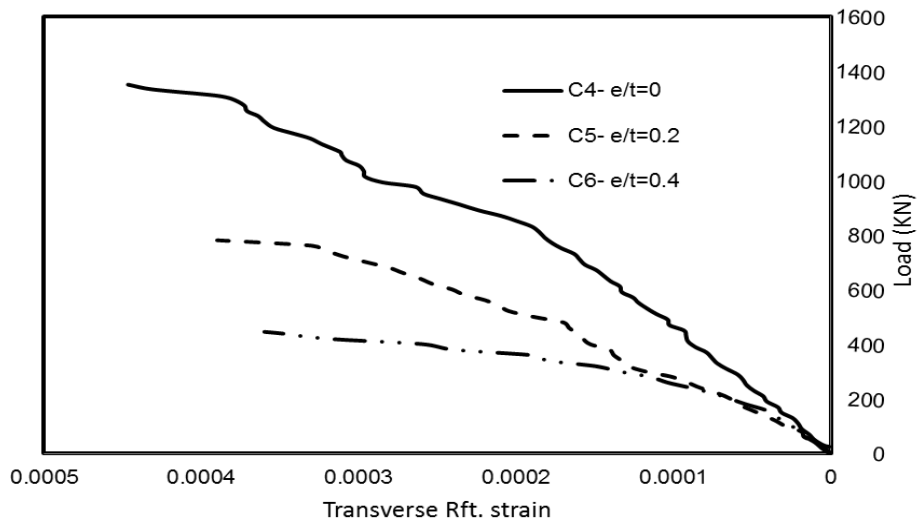


**Fig.14:** Load -transverse reinforcement Strain curve for columns with transverse reinforcement having ratio of 0.6%.

#### IV. CONCLUSIONS

This paper investigated the behavior of reinforcement lightweight concrete under uniaxial compressive stress following conclusion may be drawn:

- The average test results for two specimens indicates that the generalized stress block parameter  $k_1$  is 0.61 when cylinder lightweight concrete compressive strength 30 MPa. The generalized stress block parameter  $k_2$  is found equal 0.37. The generalized stress block parameter  $k_3$  for LWC is determined to be similar to NSC and it is equal 1.12. From those values we found the stress block parameters  $\alpha_1$  equal 0.93 and  $\beta_1$  equal 0.73.
- In case of increasing eccentricity ratio (e/t) from 0 to 0.2 the cracking load decreased by 50%, 50.4% for transverse reinforcement ratios of 0.4% and 0.6% respectively, also when increase eccentricity ratio (e/t) from 0 to 0.4 the cracking load decreased by 77%, 66.4% for transverse reinforcement ratios of 0.4% and 0.6% respectively.
- In case of increasing eccentricity ratio (e/t) from 0 to 0.2 the failure load decreased by 40.1%, 42.2% for transverse reinforcement ratios of 0.4% and 0.6% respectively. Also when increase eccentricity ratio (e/t) from 0 to 0.4 the failure load decreased by 69.6%, 67% for transverse reinforcement ratios of 0.4% and 0.6% respectively.
- In case of increasing eccentricity ratio (e/t) from 0 to 0.2 the concrete compressive strain increased by 23.5%, 18.4% for transverse reinforcement ratios of 0.4% and 0.6% respectively. Also when increase eccentricity ratio (e/t) from 0 to 0.4 the concrete compressive strain increased by 16.5%, 12.6% for transverse reinforcement ratio 0.4% and 0.6% respectively.
- In case of increasing eccentricity ratio (e/t) from 0 to 0.2 the longitudinal reinforcement strain at inner side reduced by 3%, 5.4% for transverse reinforcement ratios of 0.4% and 0.6% respectively. Also when increase eccentricity ratio (e/t) from 0 to 0.4 the longitudinal reinforcement strain at inner side increased by 9.2% for transverse reinforcement ratio 0.6%.
- In case of increasing eccentricity ratio (e/t) from 0 to 0.2 the longitudinal reinforcement strain at outer side decreased by 92.4% for transverse reinforcement ratios of 0.4%. Also when increase eccentricity ratio (e/t) from 0 to 0.4 the longitudinal reinforcement strain at outer side increased by 165.6%, 162.4% for transverse reinforcement ratios of 0.4% and 0.6% respectively.
- In case of increasing eccentricity ratio (e/t) from 0 to 0.2 the transverse reinforcement strain increased by 8.47%, 12.7% for transverse reinforcement ratios of 0.4% and 0.6% respectively. Also when increase eccentricity ratio (e/t) from 0 to 0.4 the transverse reinforcement increased by 17.5%, 19.4% for transverse reinforcement ratios of 0.4% and 0.6% respectively.
- The changes in transverse reinforcement bar diameter between 8mm (0.4%), 10 mm (0.6%). This increases in ratio of transverse reinforcement between the columns resulted to more confinement and it leads to increase the failure load, when the load increased the deformation increased and all strains increased.

#### REFERENCES

- [1]. Chandra, S. and Berntsson, L (1996). *Lightweight aggregate concrete: science, technology and applications*. Noyes Publications.
- [2]. Berra, M. and Ferrara, G. "Normal weight and total-lightweight high-strength concretes: A comparative experimental study," SP-121, 1990, pp.701-733.
- [3]. Kayali, O.A. and Haque, M.N. "A new generation of structural lightweight concrete," ACI, SP-171, 1997, pp. 569-588.
- [4]. Bai, Y. and Basheer, P.A.M. "Influence of Furnace Bottom Ash on properties of concrete," Proceedings of the Institution of Civil Engineers, Structure and Buildings 156, February 2003, Issue 1, pp. 85-92.
- [5]. Bai, Y. and Basheer, P.A.M. "Properties of concrete containing Furnace Bottom Ash as a sand replacement material," Proceedings of structural faults and repair (CD-ROM), London, July 1-3, 2003.
- [6]. Shetty.M.S., "concrete technology", (1982). 12. H.-W.Song. , "Development of structure lightweight foamed concrete using polymer foam agent" Yonsei University., Seoul 120-749, Korea
- [7]. ACI 213R-03 "guide for structural Lightweight-aggregate concrete" ACI Committee 213, American Concrete Institute, Farmington Hills, Michigan, USA, 2003.
- [8]. Zhang, M.H. Gjorv, O.E (1995), "Properties of High-Strength Lightweight Concrete", CEB/FIP International Symposium on Structural Lightweight Aggregate Concrete, Ed. I. Holand et al.,(Cited in BE96-394/R1,1989).
- [9]. Newan, J.B., (1993), "Properties of Structural Lightweight Concrete in Structural Lightweight concrete", Ed. J. L. Clarke, Blackie, Chapman & Hall, London, (19- 44), (cited in BE96-3942/R1, 1989).
- [10]. Smeplass, S. (1992), "Mechanical Properties – Lightweight Concrete Report 4.5, High Strength Concrete", SP4-Material Design, SINTEF, (Cited in BE96-3942/R1, 1989).

- [11]. Curcio, F., Galeata, D., Gallo, A., Giammatteo, M., (1998). High-Performance Lightweight Concrete for the Precast Pre-stressed Concrete Industry. Proc. 4th. Int. CANMET/ACI/JCI Symposium, To-Kushima, Japan, pp. 389-406, (Cited in BE96- 392/R1, 1989).
- [12]. Y.C. Kan, L.H. Chen, C.H. Wu, C.H. Huang, T. Yen, and W.C. Chen "Behavior and Size Effect of Lightweight Aggregate Concrete Column under Axial Load "Proceeding of the 5th Conference on Lightweight Aggregate Concrete, National Chung-Hsing University Taiwan, 2012, pp.1-20. (in Chinese).
- [13]. Chandra S., Berntsson L., *Lightweight Aggregate Concrete*, Noyes Publications, New York, 2003
- [14]. Ramachandran V.S., *Concrete Admixtures Handbook*, 2nd ed., Noyes Publications, New Jersey, 1995.
- [15]. ACI Committee 213, "Guide for Structural Lightweight Aggregate Concrete", American Concrete Institute, 1987
- [16]. Hognestad, E., Hanson, N. W., and McHenry, D., "Concrete Stress Distribution in Ultimate Strength Design," *Journal of the American Concrete Institute*, Vol. 27, No. 4, December 1955, pp. 455-479.
- [17]. Halit Cenani Mertol, "Behavior Of High-Strength Concrete Members Subjected To Combined Flexure And Axial Compression Loadings" Raleigh, North Carolina December 2006.
- [18]. R. PARK and T. PAULAY. "Reinforced Concrete Structures" department of civil engineering, University of Canterbury, Christchurch, New Zealand, 1975.
- [19]. Hussein O. Okail "flexural behavior of reinforced self-compacting lightweight concrete beams ", Faculty of engineering, Ain Shams University, 2008.
- [20]. HOSNY, AMR. "Behavior of Concrete Members Containing Lightweight Synthetic Particles", Civil Engineering, Raleigh, NC, 2010.
- [21]. Eethar Th. Dawood and Mahyuddin Ramli "Rational Mix Design of Lightweight Concrete for Optimum Strength "2nd International Conference on Built Environment in Developing Countries (Icedc 2008).